

## CROSS SECTION MEASUREMENTS OF FAST NEUTRONS WITH ISOTOPES OF MERCURY

**M. Al-Abyad<sup>1,2</sup>, S. Sudár<sup>1†</sup>, M.N.H. Comsan<sup>2</sup> and S.M. Qaim<sup>1</sup>**

<sup>1</sup>*Institut für Nuklearchemie, Forschungszentrum Jülich GmbH, D-52425 Jülich,  
Germany*

<sup>2</sup>*Cyclotron Facility, Nuclear Research Center, Atomic Energy Authority, Cairo  
13759, Egypt*

### Abstract

Cross section were measured for the reactions  $^{196}\text{Hg}(n,2n)^{195}\text{Hg}^{\text{m,g}}$ ,  $^{198}\text{Hg}(n,2n)^{197}\text{Hg}^{\text{m,g}}$ ,  $^{204}\text{Hg}(n,2n)^{203}\text{Hg}$ ,  $^{198}\text{Hg}(n,p)^{198}\text{Au}^{\text{g}}$  and  $^{199}\text{Hg}(n,p)^{199}\text{Au}$  over the neutron energy range of 7.6 - 12.5 MeV. Quasimonoenergetic neutrons were produced via the  $^2\text{H}(d,n)^3\text{He}$  reaction using a deuterium gas target at the Jülich variable energy compact cyclotron CV 28. Use was made of the activation technique in combination with high-resolution HPGe-detector  $\gamma$ -ray spectroscopy. All the data were measured for the first time over the investigated energy range. The transition from the present low- energy data to the literature data around 14 MeV is generally good. Nuclear model calculations using the codes STAPRE and EMPIRE-2.19 which employ the statistical and precompound model formalisms were undertaken to describe the formation of both the isomeric and ground states of the products. The total reaction cross section of a particular channel is reproduced fairly well by the model calculations, with STAPRE giving slightly better results.

<sup>†</sup>*Permanent address: Institute of Experimental Physics, University of Debrecen, H-4010 Debrecen, Hungary.*

### I. INTRODUCTION

Studies of excitation functions of neutron threshold reactions are of considerable importance for testing nuclear models as well as for practical applications. We chose to study the neutron-induced reactions on isotopes of mercury mainly due to two reasons. Firstly, mercury is being considered as a target material in spallation neutron sources. The (n,xn) reaction cross sections of mercury isotopes are therefore important for calculations on neutron multiplication. Secondly,  $^{195}\text{Hg}^{\text{m}}$  and  $^{197}\text{Hg}^{\text{m}}$  are high-spin isomers (each having a value of  $13/2^-$ ) as compared to the respective ground state (with spin  $1/2^-$ ). The relative formation of those states in (n,2n) reactions as a function of the incident neutron energy should thus be very interesting.

A literature survey showed that for the isotopes of mercury almost no experimental information is available for neutron-induced reactions from their thresholds up to 12.5 MeV. Most of the data existing in the literature were measured at neutron energies around 14 MeV [1-9]. The only

exception is the  $^{198}\text{Hg}(n,2n)^{197}\text{Hg}^m$  reaction, where Kiraly et al [10] reported data for two neutron energies, namely 11.2 and 12.5 MeV. The aim of this work was to determine the excitation functions of several neutron-induced reactions on isotopes of mercury near their thresholds and to compare them with the results of nuclear model calculations, with particular attention to the formation of the isomeric states.

## II. EXPERIMENT

Cross sections were measured by activation and identification of the radioactive products. This technique is very suitable for investigating low-yield reaction products and closely spaced low-lying isomeric states, provided their lifetimes are not too short. The details have been described over the years in many publications from Jülich [cf. Ref. 11-17]. Here we give some salient features relevant to the present measurements.

### A. Samples and Irradiations

About 5 g of  $\text{HgCl}_2$  powder of natural isotopic composition (99.9% pure, provided by Chempur or ABCR GmbH, Germany) was pressed at  $10\text{ ton/cm}^2$  and a pellet (2.0 cm diameter, 0.3 cm thick) was obtained. Each pellet was placed in an aluminum capsule, the total thickness of each sample, including the capsule, was 0.62 cm. Monitor foils Al (200  $\mu\text{m}$  thick) and Fe (100  $\mu\text{m}$  thick) of the same diameter as the capsule were then attached in front and at the back of each sample.

Irradiations were performed at the Jülich variable energy compact cyclotron CV 28. The quasi-monoenergetic neutrons were produced via the  $^2\text{H}(d,n)^3\text{He}$  reaction ( $Q = 3.27\text{ MeV}$ ) on a  $\text{D}_2$  gas target (3.7 cm long,  $1.8 \times 10^5\text{ Pa}$  pressure). A sketch of the target is shown in Fig.1. The characteristics of this neutron source have been described earlier [11,18,19]. The samples were placed in the  $0^\circ$  direction relative to the incident deuteron beam, at a distance of 1.0 cm from the beam stop. By changing the deuteron energy between 5.0 and 10.0 MeV, it was possible to obtain neutrons of energies between 7.5 and 12.5 MeV. The beam current was kept constant at 2-3  $\mu\text{A}$ . The time of irradiation varied between 5 and 6 h. At each energy two irradiations were done, one with the target filled with the  $\text{D}_2$  gas and the other as empty (gas in/gas out). This allowed a correction for the activity formed from the background neutrons.

### B. Neutron Energies and Flux Densities

The average neutron energy effective at each sample was calculated using the Monte Carlo program NEUT [20,21] which takes into account the energy loss of the deuteron in the gas cell and the foils. The breakup of the deuteron on the  $\text{D}_2$  gas was determined according to the results of Cabral et al [22]. The program NEUT was also used to calculate the whole neutron spectrum which is divided in a breakup part and a monoenergetic part. The ratio of the activity induced by the monoenergetic neutrons to that by the breakup neutrons was calculated and used for the correction of the contribution of the breakup neutrons. The correction was of the order of a few percent, depending on the reaction threshold and the excitation function of the investigated reaction. An accurate measurement of the deuteron energy was performed completely on line; a personal computer controlled the position of the probe and evaluated the signal produced by the HF detector electronics [23]. The diameter of the beam falling on the front of the neutron target was 4 mm. For ascertaining the constancy of the neutron flux, a constant check of the  $\text{D}_2$  gas pressure in the cell and of the deuteron beam current on the target was performed. The neutron flux density effective during each irradiation was determined via two monitor reactions, namely  $^{56}\text{Fe}(n,p)^{56}\text{Mn}$  ( $T_{1/2} = 2.58\text{ h}$ ,  $E_\gamma = 847\text{ keV}$ ,  $I_\gamma = 98.9\%$ ), and  $^{27}\text{Al}(n,\alpha)^{24}\text{Na}$  ( $T_{1/2} = 14.97\text{ h}$ ;  $E_\gamma = 1369\text{ keV}$ ;  $I_\gamma = 100\%$ ). The cross sections of the monitor reactions were taken from the IRDF (2002) computer file

[cf. Ref.24].The flux densities were calculated after correction of monitor product activities from background neutrons. The average flux density effective on each sample was then obtained by taking the mean value of the calculated flux density for the front and back foils.

### C. Measurement of Radioactivity

The activation products were identified by  $\gamma$ -ray counting and checking their half-lives. Table 1 gives the reactions investigated, their Q-values and the decay data of the products [25-26] used in the quantitative assay of the activity. For measurements HPGe detectors were used. The samples and monitor foils were placed either directly on the end cap of the detector or at a distance of 5 cm. The peak area analysis was done using the software GAMMAVISION, version 5.10, EG&G ORTEC. The detector efficiency was determined experimentally using a selected set of  $\gamma$ -ray standard sources obtained from Amersham International or PTB Braunschweig. The count rate of each  $\gamma$ -ray was corrected for coincidence summing effect, geometric effect of the  $\text{HgCl}_2$ -sample, and  $\gamma$ -ray self-attenuation in the sample.

Correction for the  $\gamma$ -ray attenuation in the  $\text{HgCl}_2$  sample was carefully calculated. Furthermore, in order to determine the counting efficiency for the extended source placed directly on the end cap of the detector, a radioactive source especially prepared was used as in two earlier cases [28,29]. For this purpose, 10 mg each of  $\text{HgCl}_2$  and  $\text{Eu}_2\text{O}_3$  was irradiated using a 14 MeV d(Be) neutron source, and the induced activity in each sample was assayed via  $\gamma$ -ray spectrometry. The sample to detector distance was 10 cm. Thereafter the irradiated samples were thoroughly mixed with about 5 g of  $\text{HgCl}_2$  in a mortar. The mixture was then pressed to a pellet and placed in the Al capsule, as in the case of the sample for irradiation. A  $\gamma$ -ray spectrometric analysis of thus prepared sample gave the effective efficiency of the detector for  $\gamma$ -rays of various energies.

In the case of  $^{204}\text{Hg}(n,2n)^{203}\text{Hg}$  and  $^{198}\text{Hg}(n,2n)^{197}\text{Hg}^{\text{m,g}}$  reactions special care was necessary to correct for the effective background activity via the  $^{202}\text{Hg}(n,\gamma)^{203}\text{Hg}$  and  $^{196}\text{Hg}(n,\gamma)^{197}\text{Hg}^{\text{m,g}}$  processes. For this purpose two procedures were applied. In the first method, the gas-out measurement gave the (n, $\gamma$ ) contribution from the background neutrons of energies up to about 2MeV. The (n, $\gamma$ ) from the faster neutrons was estimated using the calculated D-D neutron spectrum (from NEUT, see above) and the  $^{196}\text{Hg}(n,\gamma)$  or  $^{202}\text{Hg}(n,\gamma)$  excitation function reported in the literature [27]. Due to low cross section of the (n, $\gamma$ ) over the energy range of 2 to 13 MeV (decreasing from 10 mb to about 1mb),the latter contribution is much smaller than the former contribution. In the second method, irradiations were done also with neutrons of energies just below the threshold of the two investigated (n,2n)reactions. The product radioactivity was then assumed to be due to the disturbing (n, $\gamma$ ) reaction. A further very small but slightly increasing contribution of the (n, $\gamma$ ) process with the increasing neutron energy was estimated via the calculational method described above. In general, the correction data from the two procedures agreed within a few percent. The final result was that contribution of the  $^{202}\text{Hg}(n,\gamma)^{203}\text{Hg}$  to the formation of  $^{203}\text{Hg}$  was about 30%; in the case of  $^{197}\text{Hg}^{\text{m,g}}$ , however, the contribution of the  $^{196}\text{Hg}(n,\gamma)^{197}\text{Hg}^{\text{m,g}}$  reaction turned out to be negligibly small.

### D. Calculation of Cross Sections and Their Uncertainties

The count rates at the end of bombardment (EOB), after corrections for contributions from background neutrons, were converted to decay rates by introducing corrections for summing effects, gamma ray emission intensity and the efficiency of the detector. Cross sections were then calculated using the well-known activation equation.

The individual uncertainties in cross section measurements using D-D neutrons have been described in several publications [cf. Refs. 11-17]. The uncertainty in the excitation function of the monitor reaction was taken as 4% and that in the averaging of the neutron flux as 5%. The efficiency of the  $\gamma$ -ray detector (incorporating self-absorption, geometry, and pileup) had an uncertainty of about 6%. The uncertainty in the decay data used was <2%. Besides these systematic uncertainties, the major random uncertainties involved were due to counting statistics (2-5%),  $\gamma$ -ray peak area analysis (2-15%) and corrections for contributions from background neutrons (2-10%). Because of low count rates the uncertainties in counting statistics and peak area analysis were relatively large in the low neutron energy region. In the high neutron energy range of 10-12 MeV, those two uncertainties were much lower, and the major source of uncertainty was the correction due to the background neutrons. The total uncertainty in each cross section value was obtained by combining all the individual uncertainties in quadrature it amounted to be 20%.

### III. RESULTS AND DISCUSSION

#### A. Cross Sections and Excitation Functions

The cross sections measured over the energy range of 7.6 to 12.5 MeV are given in Table 2. Except for two data points at 11.2 and 12.5 MeV for the  $^{198}\text{Hg}(n,2n)^{197}\text{Hg}^m$  reaction [10], all the data reported in this work in the above mentioned energy range have been determined for the first time. The various reactions investigated are discussed below.

#### $^{196}\text{Hg}(n,2n)^{195}\text{Hg}^{m,g}$

The irradiated sample was counted immediately after EOB to determine the independent formation cross section of  $^{195}\text{Hg}^g$  ( $T_{1/2}= 9.9$  h). After a decay time of about 50 h it was counted again to measure the activity of  $^{195}\text{Hg}^m$  ( $T_{1/2}= 41.6$  h). The present cross-section data are shown in Figs. 2 and 3 as a function of the neutron energy, together with the literature data around 14 MeV [4,5,7]. The transition from the low-energy region to higher energy region is smooth; only a few data points in the 14 MeV region do not fit into the general trend (cf. the value for  $^{195}\text{Hg}^m$  by Temperley [4] and the one for  $^{195}\text{Hg}^g$  by Hankla et al [5]). The results of the two nuclear model calculations, namely STAPRE and EMPIRE 2.19 [29,30,33], reproduce the experimental excitation function of the  $^{196}\text{Hg}(n,2n)^{195}\text{Hg}^m$  reaction very well. In the case of the  $^{196}\text{Hg}(n,2n)^{195}\text{Hg}^g$  reaction, whereas the STAPRE calculation reproduces the experimental excitation function very well, the EMPIRE results in the energy range above 12.5 MeV are rather low.

#### $^{198}\text{Hg}(n,2n)^{197}\text{Hg}^{m,g}$

The first measurement in this case was also done immediately after EOB to determine the independent formation cross section of  $^{197}\text{Hg}^m$  ( $T_{1/2}= 23.8$  h). Thereafter, measurement was done about one week after EOB to determine the activity of  $^{197}\text{Hg}^g$  ( $T_{1/2}= 64.1$  h); the contribution via the decay of  $^{197}\text{Hg}^m$  was then subtracted.

The present results are shown in Figs. 4 and 5 together with the literature data [4-7,10], mainly in the energy region around 14 MeV. Again the transition from the low-energy to higher energy region is smooth; however, our results for  $^{197}\text{Hg}^m$  are considerably lower than the data by Kiraly et al [10]. The results of the two nuclear model calculations differ appreciably from each other in some energy regions. For  $^{197}\text{Hg}^m$ , in the low energy region the EMPIRE calculation appears to be in better agreement with our data. In the case of  $^{197}\text{Hg}^g$ , near the threshold the STAPRE results are somewhat higher than the experimental data and the EMPIRE results are lower.

$^{204}\text{Hg}(n,2n)^{203}\text{Hg}$ 

In the study of this reaction a subtraction of the  $^{202}\text{Hg}(n,\gamma)^{203}\text{Hg}$  contribution was necessary. We determined this contribution by a careful analysis of the gas in/gas out data and taking into account a correction for the breakup background neutrons. Furthermore, the measurement of the sample was started about one week after EOB and continued for several weeks. This was necessary to avoid the disturbance from the 23.8 h  $^{197}\text{Hg}^{\text{m}}$  which emits a  $\gamma$ -ray in the vicinity of the 279 keV  $\gamma$ -ray used for the assay of  $^{203}\text{Hg}$ .

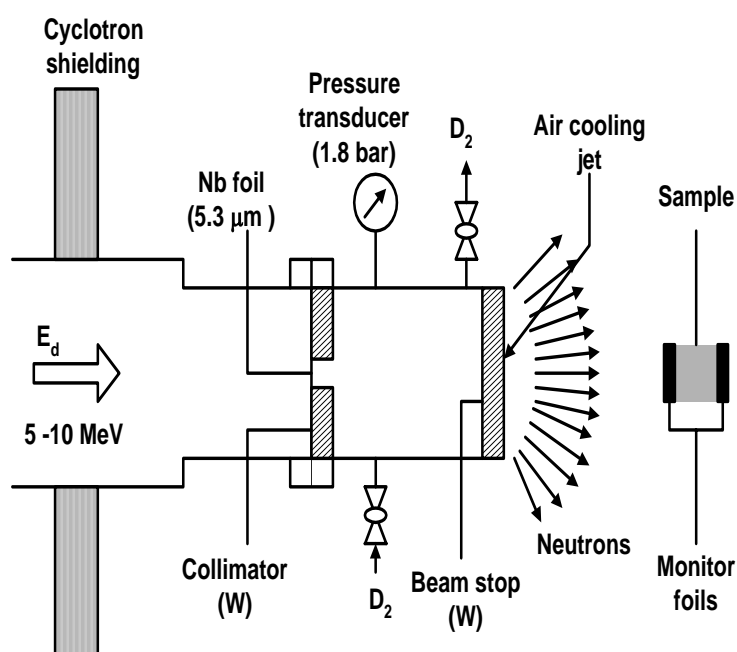
The results obtained are shown in Fig. 6 together with the literature data in the energy range of 13-18 MeV [1-7]. Again the transition from the low-energy to higher energy region is smooth. The data base seems to be now established. The results of nuclear model calculations reproduce the experimental data rather well, except for the region beyond the maximum of the excitation function. In particular the EMPIRE results are too high.

**Table 1.** Nuclear reactions studied and decay data of the products.

Nuclear reaction	Q- Value (MeV)	Mode of decay (%)	Half- life	$E_{\gamma}$ (keV)	$I_{\gamma}$ (%)
$^{196}\text{Hg}(n,2n)^{195}\text{Hg}^{\text{g}}$	- 8.84	EC (100)	9.9 h	779.8	7.0
$^{196}\text{Hg}(n,2n)^{195}\text{Hg}^{\text{m}}$	-9.05	IT (54)	41.6 h	261.8	37.9
		EC (46)		560.3	7.5
$^{198}\text{Hg}(n,2n)^{197}\text{Hg}^{\text{g}}$	- 8.49	EC (100)	64.14 h	77.3	18.7
				191.4	0.63
$^{198}\text{Hg}(n,2n)^{197}\text{Hg}^{\text{m}}$	-8.56	IT (91.4) EC (8.6)	23.8 h	134	33.0
$^{204}\text{Hg}(n,2n)^{203}\text{Hg}$	-7.50	$\beta^-$ (100)	46.6 d	279.2	81.5

**Table 2.** Activation cross sections determined in this work.

$\langle E_n \rangle$ (MeV)	Cross section (mb)				
	$^{196}\text{Hg}(n,2n)^{195}\text{Hg}^g$	$^{196}\text{Hg}(n,2n)^{195}\text{Hg}^m$	$^{198}\text{Hg}(n,2n)^{197}\text{Hg}^g$	$^{198}\text{Hg}(n,2n)^{197}\text{Hg}^m$	$^{204}\text{Hg}(n,2n)^{203}\text{Hg}$
7.66±0.22					11.5±2
8.45±0.25					263±48
9.73±0.28	60±11	161±30	233±43	128±23	846±155
10.59±0.31	385±71	281±51	500±92	304±56	1071±197
11.07±0.34	444±81	385±70	655±120	405±74	1285±236
11.25±0.34	554±102	507±93	848±156	400±73	1584±291
11.51±0.34	662±121	591±108	692±127	518±95	1665±306
11.92±0.35	780±1432	570±104	811±149	535±98	1495±275
12.40±0.36	786±144	862±158	870±160	540±99	1721±316
12.53±0.50	923±170	990±182	955±175	667±122	1903±350

**Fig. 1.** Sketch of deuterium gas target used to produce quasi-monenergetic neutrons

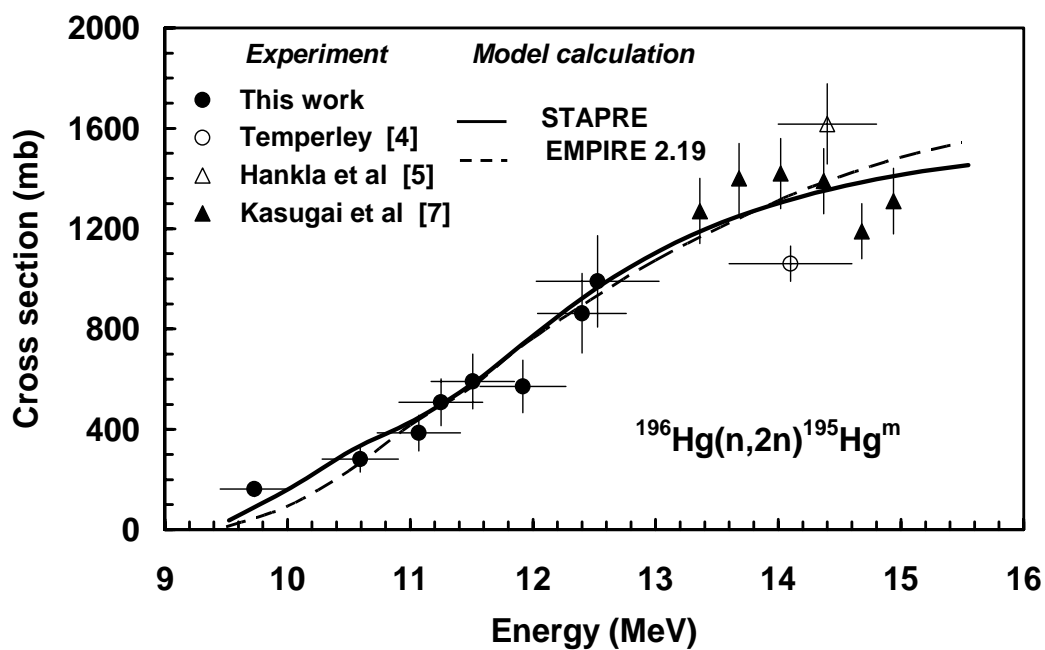


Fig. 2. Excitation function of the  $^{196}\text{Hg}(n,2n)^{195}\text{Hg}^m$  reaction.

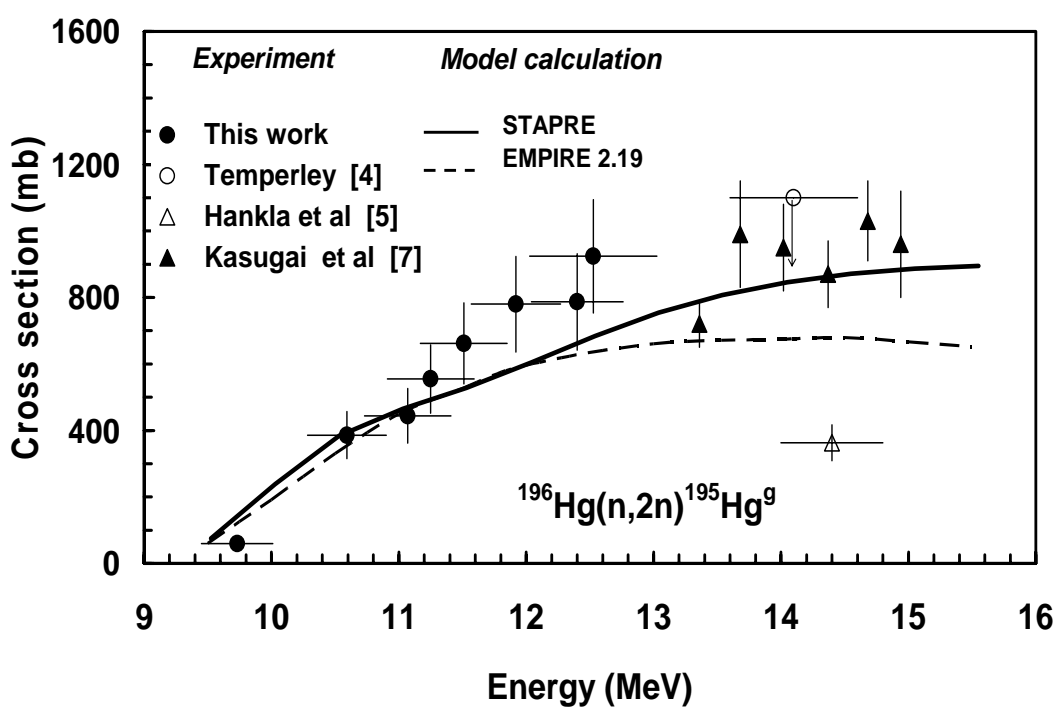


Fig. 3. Excitation function of the  $^{196}\text{Hg}(n,2n)^{195}\text{Hg}^g$  reaction.

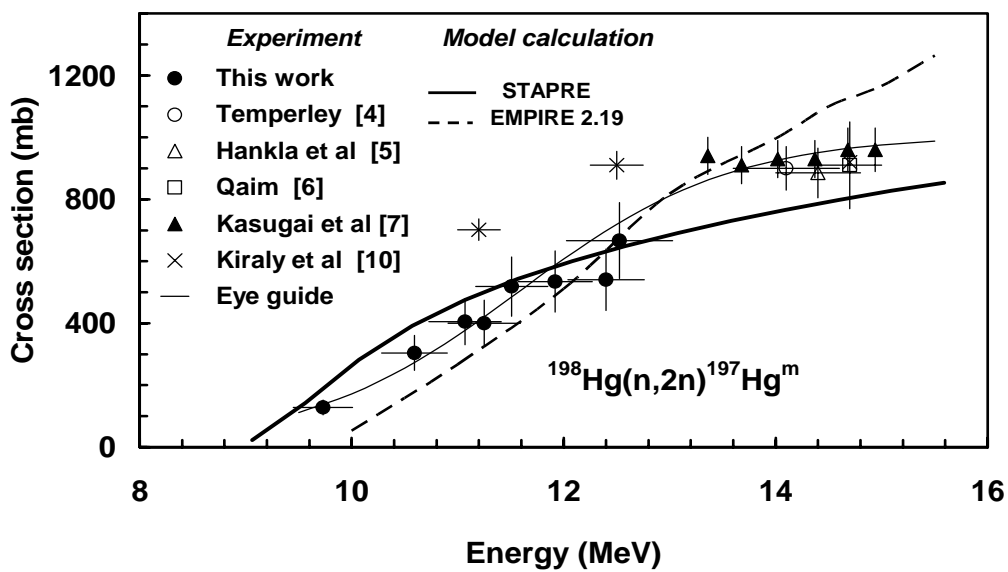


Fig. 4. Excitation function of the  $^{198}\text{Hg}(n,2n)^{197}\text{Hg}^m$  reaction.

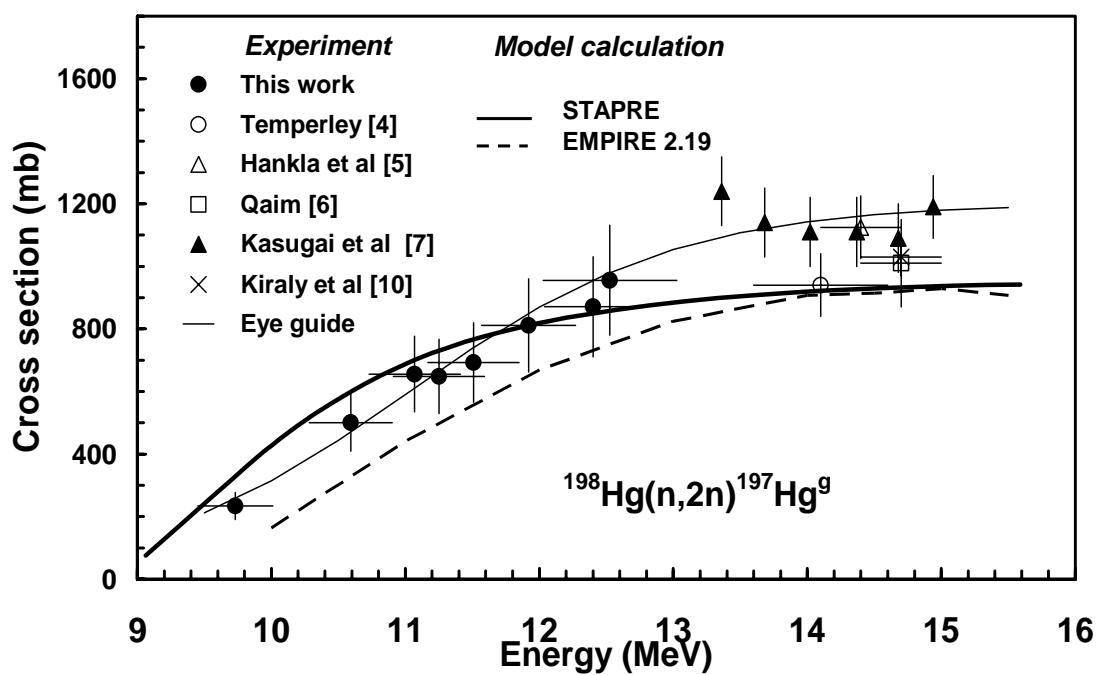


Fig. 5. Excitation function of the  $^{198}\text{Hg}(n,2n)^{197}\text{Hg}^g$  reaction.

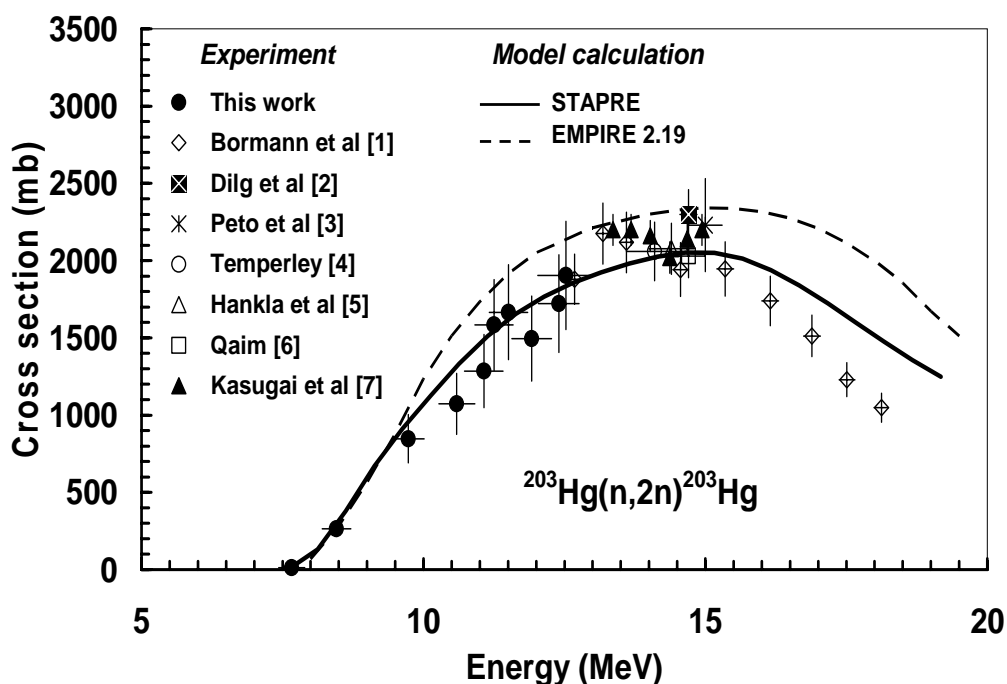


Fig.6. Excitation function of the  $^{204}\text{Hg}(n,2n)^{203}\text{Hg}$  reaction.

## V. CONCLUSION

Experimental results reported in this work should provide a good database for the (n,2n) reactions on several isotopes of mercury, especially with regard to calculations on neutron multiplication while using mercury as a target material in a spallation neutron source. Nuclear model calculations using the codes STAPRE and EMPIRE 2.19 showed that the total reaction cross section of a particular channel under consideration is reproduced fairly well by the Hauser-Feshbach formalism including precompound effects, with STAPRE giving slightly better results.

## ACKNOWLEDGEMENTS

We thank Prof. H.H.Coenen for his support of this work, the crew of the compact cyclotron CV 28 at Jülich for performing the irradiations, and S. Sepellerberg for experimental assistance. This work was done under a German-Egyptian bilateral research cooperation and we are grateful to the concerned authorities in both countries for their support.

## REFERENCES

- (1) M. Bormann, H.-K. Feddersen, H.-H. Holscher, W. Scobel, and H. Wagner, *Zeitschrift fuer Physik A* **277**, 203 (1976).
- (2) W. Dilg, H. Vonach, G. Winkler, and P. Hille, *Nucl. Phys.* **A118**, 9 (1968).
- (3) G. Petö, P. Bornemisza-Pausperthl, and J. Karolyi, *Acta Physica Hungarica* **25**, 91 (1968).
- (4) J. K. Temperley, *Phys. Rev.* **178**, 1904 (1969).
- (5) A. K. Hankla, R. W. Fink, and J. H. Hamilton, *Nucl. Phys.* **A180**, 157 (1972).
- (6) S. M. Qaim, *Nucl. Phys.* **A185**, 614 (1972).

- (7) Y. Kasugai, F. Maekawa, Y. Ikeda, and H. Takeuchi, *J.Nucl.Sci.Technol.* **38**, 1048 (2001).
- (8) EXFOR, Nuclear reaction data, EXFOR is accessed on line at <http://www.nndc.bnl.gov/nndc/exf> or [www.nea.fr/www-nds.iaea.org/exfor](http://www.nea.fr/www-nds.iaea.org/exfor), (2003).
- (9) CINDA-A, The Index to Literature and Computer Files on Microscopic Neutron Data, IAEA, Vienna, 1990; CINDA 2000, The Index to Literature and Computer Files on Microscopic Neutron Data, IAEA, Vienna, (2003).
- (10) B. Király, J. Csikai, and R. Doczi, Proceedings of the 2000 Symposium on Nuclear Data, November 16-17, 2000, JAERI, Tokai, Japan **JAERI-C-283**, (2001).
- (11) S.M. Qaim, R. Wölfle, M.M. Rahman, and H. Ollig, *Nucl. Sci. Eng.* **88**, 143 (1984).
- (12) M.M. Rahman and S.M. Qaim, *Nucl. Phys.* **A435**, 43 (1985).
- (13) M. Ibn-Majah and S.M. Qaim, *Nucl. Sci. Eng.* **104**, 271 (1990).
- (14) I.-G. Birn and S.M. Qaim, *Nucl. Sci. Eng.* **116**, 125 (1994).
- (15) M. Bostan and S.M. Qaim, *Phys. Rev.* **C49**, 266 (1994).
- (16) F. Cserpák, S. Sudár, J. Csikai, and S.M. Qaim, *Phys. Rev.* **C 49**, 1525 (1994).
- (17) C.D. Nesaraja, S. Sudár, and S. M. Qaim, *Phys. Rev.* **C 68**, 024603 (2003).
- (18) A. Grallert, J. Csikai, S.M. Qaim, and J. Knieper, *Nucl. Instrum. Methods Phys. Res.* **A334**, 154 (1993).
- (19) A. Grallert, J. Csikai, and S.M. Qaim, *Nucl. Instrum. Methods Phys. Res.* **A337**, 615 (1994).
- (20) I.-G. Birn, Kernforschungsanlage Jülich, internal Report No. **INC-IB-1**, (1992).
- (21) I.-G. Birn, CEC-JRC, IRMM, Geel, internal Report No. **GE/R/VG/85/94**, (1994).
- (22) S. Cabral, B. Börker, H. Klein, and W. Mannhart, *Nucl. Sci. Eng.* **106**, 308 (1990).
- (23) Z. Kormány, *Nucl. Instrum. Methods Phys. Res.* **A337**, 258 (1994).
- (24) International Reactor Dosimetry File: IRDF-2002, available online at <http://www-nds.iaea.org/irdf2002>.
- (25) R. B. Firestone, *Table of Isotopes*, Wiley, New York (1996).
- (26) J. Kopecky, Atlas of neutron capture cross sections, Report INDC(NDS)-362, International Atomic Energy Agency, Vienna, 1997.
- (27) R.M. Klopries, R. Doczi, S. Sudár, J. Csikai, and, S.M. Qaim, *Radiochim. Acta* **76**, 3 (1997).
- (28) C. Nesaraja, K.-H. Linse, S. Spellerberg, S. Sudar, A. Suhaimi, and S.M. Qaim, *Radiochim. Acta* **86**, 1 (1999).
- (29) M.Uhl and B. Strohmaier, Computer Code for Particle Induced Activation Cross Section and Related Quantities, Institut für Radiumforschung und Kernphysik, Vienna, (1976).
- (30) O. Bersillon, Un programme de modele optique spherique Centre d'Etudes de Bruyères-le Châtel, Paris, (1981).
- (31) J. C. Ferrer, J. D. Carlson, and J. Rapaport, *Nucl. Phys.* **A 275**, 125 (1977).
- (32) W. Dilg, W. Schantl, and H. Vonach, *Nucl. Phys.* **A217**, 216 (1973).
- (33) M. Herman, R. Capote, B. Carlson, P. Oblozinsky, M. Sin, A. Trakov, and V. Zerkin, EMPIRE-II, Nuclear reaction model code, IAEA, version 2.19 (2005).